The Maximum Number of Cells With Modulated Binary Sensors

Longxiang Luo, *Member, IEEE*, Yang Xiao, *Fellow, IEEE*, and Wei Liang, *Senior Member, IEEE*

***Abstract*—Due to the low cost and good privacy protection of binary sensors, there are many applications of binary sensors. To enhance the spatial awareness of binary sensors, researchers utilize modulators to modulate views of sensors into visible and invisible regions so that the monitoring space is segmented into small cells identified by signatures. When a warm object moves in these cells, its location or moving trajectory can be acquired more accurately with modulators than without modulators. Accordingly, the maximum number of cells (MNC) in a deployment determines partially the maximal spatial awareness of the binary sensor system. In this paper, we provide a theoretical study of the MNC, given the number of sensors and the number of modulators. We also find the sufficient and necessary conditions to achieve the MNC so that we provide the reasons why deployment cannot obtain the MNC. These conditions can guide researchers to design the MNC deployments. Furthermore, we provide a method to calculate the number of cells when a deployment sometime cannot obtain the MNC. Our experiments provide deep insights into the influences of those conditions on the MNC and the MNC on the spatial awareness of binary sensor systems.**

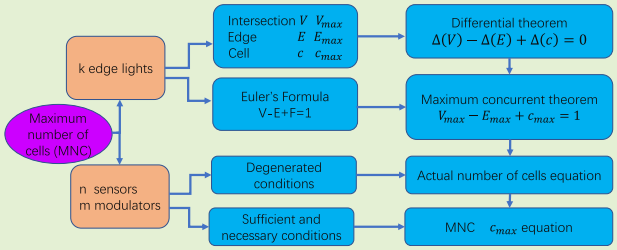

***Index Terms*—Internet of Things (IoT), binary sensors, sensor deployment, sensor array, spatial awareness, the maximum number of cells.**

Manuscript received November 14, 2020; revised January 26, 2021; accepted February 6, 2021. Date of publication February 18, 2021; date of current version April 5, 2021. The work of Longxiang Luo and Wei Liang was supported in part by the National Key Research and Development Program of China under Grant 2017YFE0123000, in part by the National Natural Science Foundation of China under Grant 62022088, in part by the International Partnership Program of Chinese Academy of Sciences under Grant 173321KYSB20180020 and Grant 173321KYSB20200002, in part by the Liaoning Provincial Natural Science Foundation of China under Grant 2019-YQ-09 and Grant 2020JH2/10500002, and in part by the LiaoNing Revitalization Talents Program under Grant XLYC1902110. The associate editor coordinating the review of this article and approving it for publication was Dr. Prosanta Gope. *(Corresponding authors: Yang Xiao; Wei Liang.)*

Longxiang Luo is with the State Key Laboratory of Robotics, Shenyang Institute of Automation, Chinese Academy of Sciences, Shenyang 110016, China, also with the Key Laboratory of Networked Control Systems, Chinese Academy of Sciences, Shenyang 110016, China, also with the Institutes for Robotics and Intelligent Manufacturing, Chinese Academy of Sciences, Shenyang 110169, China, and also with the University of Chinese Academy of Sciences, Beijing 100049, China (e-mail: luolongxiang@sia.cn).

Yang Xiao is currently with the Department of Computer Science, The University of Alabama, Tuscaloosa, AL 35487 USA (e-mail: yangxiao@ieee.org).

Wei Liang is with the State Key Laboratory of Robotics, Shenyang Institute of Automation, Chinese Academy of Sciences, Shenyang 110016, China, also with the Key Laboratory of Networked Control Systems, Chinese Academy of Sciences, Shenyang 110016, China, and also with the Institutes for Robotics and Intelligent Manufacturing, Chinese Academy of Sciences, Shenyang 110169, China (e-mail: weiliang@sia.cn).

Digital Object Identifier 10.1109/JSEN.2021.3060059

I. Introduction

BINARY wireless sensors have been utilized in many applications such as ambient assisted living [1], [2], target localization [3], object tracking [4], [5], human activity recognition [6], [8]–[10], [26], and Internet of Things (IoTs). Binary sensors are utilized to detect undesired intrusions, to locate intruder positions, to depict moving trajectories, or to identify behavior transitions (such as walk, jog, run, sit, and fall). One advantage of binary sensors is that they are very cheap and the processing overhead is very low [7]. However, since binary sensors output binary digits 0 or 1, they can neither provide enough information to distinguish absolute locations nor track the trajectories of moving objects. Reference structure tomography (RST) [11] is proposed to enhance binary sensor spatial awareness by modulating the sensing view of sensors and encoding the field of interest (FOI) with opaque modulators. With RST, the sensing view of a sensor can be partitioned into visible regions and invisible regions. Combining the monitoring results of all the sensors with modulators, we can segment the FOI into cells (subregions) coded with signatures [12] which are sequences of binary sensor states [13]. When a warm object moves in the FOI, its location and trajectory can be acquired by the binary sensor system [14].

According to [15], [16], studies of binary sensors without RST have a locating or tracking error upper bound as $\Omega(1/(\rho\gamma^{d-1}))$, where ρ is the sensor density (the number of sensors in per unit area), γ is the sensing radius of a sensor, and d is the space dimension (for a 2-dimension plane, i.e., $d = 2$). For a fixed locating or tracking error upper bound, the locating or tracking accuracy is limited by ρ and γ. Most of the studies would rather deploy as many sensors as possible (namely, a large ρ in the FOI) than change sensing radiuses γ as large as possible to obtain a better locating or tracking accuracy [20]. For instance, researchers can utilize optical devices that collect the infrared rays emitted by a warm object to enlarge the sensing radius of infrared binary sensors. Indeed, as the sensing radius increases, researchers seem to get less information from an individual sensor: its binary digit '1' localizes the target in a larger area [15]. With RST segmenting the FOI into cells, the binary sensor system localizes the target in a cell whose area can be modulated by modulators. Studies show that binary sensor systems with RST can achieve a better tracking and localization precision than studies without RST [5], [6], [8], [9], [17]. In other words, RST facilitates localization and tracking studies of binary sensors with fewer sensors than studies without RST, even though binary sensors have large sensing radiuses.

The detection and identification of targets are influenced by many factors such as the modulator shapes, the velocities, and the distances between sensors and human targets [6], [18]. The influences of the shape, the size, and the number of modulators on the shape, the size, and the number of generated cells are listed as follows.

- Modulator shapes affect the cell shapes. There are two reasons as follows. First, an invisible region is the projection of a modulator and is usually sandwiched between two visible regions and vice versa. Second, cell shapes are generated by the interlacement of invisible regions and visible regions generated by different sensors.
- The sizes of modulators affect the cell sizes. The distance between two adjacent modulators determines the size of a visible region. Furthermore, both the visible region sizes and the invisible region sizes have impacts on the cell sizes.
- The number of modulators can regulate and control the number of cells. The number of cells depends on the number of interlaced invisible and visible regions because two interlaced visible regions generate at least one cell. Deploying multiple modulators to modulate a sensor can add the visible regions and the invisible regions [19].
- Furthermore, one sensor can sense many cells with small average cell areas. In other words, the spatial awareness of binary sensors is enhanced by RST which modulates the sensing views of the sensors.

With modulators, we can repeatedly utilize a sensor to monitor and code multiple cells which enhance the spatial awareness of binary sensors in a deployment [14]. To improve the spatial awareness of binary sensors as much as possible, we need a deep understanding of the system. However, there are few theoretical studies on binary sensors with multiple modulators. In this paper, we conduct theoretical studies of the maximum number of cells (MNC) with multiple modulators. Contributions of this paper are summarized as follows:

- We conduct the theoretical study of the MNC. We also propose a method to calculate the MNC. Even though some researchers have designed many deployments of modulators and sensors [5], [6], [8], [9], they have not studied the MNC and the number of cells produced in their deployment is much smaller than the MNC. Such a small number of cells limits the spatial awareness of binary sensors.
- We study three scenarios in that deployments cannot obtain the MNC. Moreover, we propose a method to calculate the actual numbers of cells. Our study can guide researchers to reasonably select the number of modulators and to improve the precision of applications such as tracking and localization. Even though their deployments cannot achieve the MNC, researchers can utilize our proposed method to calculate the number of generated cells easily.
- We study the sufficient and necessary conditions for deployment to obtain the MNC. These conditions can be utilized as rules to design deployments or judge whether a deployment achieves the MNC or not.
- We systematically and comprehensively study the relationships of edges, intersections, and cells in the FOI. First, an application format of Euler's Formula is provided to analyze the relationships. Second, a differential parameter is defined to measure the difference values between the maximum number of intersections, edges, and cells and their actual generated numbers in the FOI. We prove that the maximum numbers of intersections, edges, and cells also satisfy the Euler's Formula, and this means they can achieve their maximum values in one deployment.
- Modulators have a significant influence on the number of cells generated in the FOI. In our experiments, we present such influence by drawing the curves hidden in theoretical studies and we study the statistical distribution of the number of modulators to impact the MNCs.

The rest of this paper is organized as follows. Section II presents the problem definition. Section III provides the theoretical studies on the MNC. In Section IV, we study the influences of the MNC on the spatial awareness of a binary sensor system with experiments. Section V introduces the related works of this paper. In Section VI, we conclude and discuss future works.

II. Problem Definition

A. Definitions and Assumptions

We study the maximum number of cells (MNC) for segmenting the FOI with n sensors and each sensor is modulated by one or multiple modulators (show in Fig. 1). As illustrated in Fig. 1, the FOI is a field or region monitored by sensors and modulators, where warm objects appear and disappear [14]. The FOI is a disc with radius R and the circle with radius R called the boundary of the FOI. Each sensor is deployed around the FOI with one or multiple modulators deployed

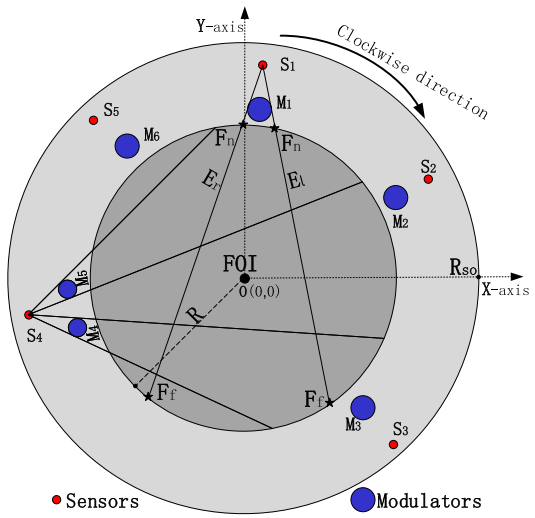

Fig. 1. Geometric relationship of default settings.

between it and the FOI. Modulators are made of opaque plastics to occlude the view of sensors and are designed into many shapes. In this paper, all of the modulators are the same size and sensors have the same device parameters. Moreover, the shape of a modulator is a disc with radius r in the 2-dimension plane.

An edge light (denotes as E) is an infrared light that cuts across the FOI, is emitted by a warm object and is tangent to a modulator [14]. Suppose that we stand at the center of a modulator in Fig. 1 (for example M_1) and face to the circle center O of the FOI. For the two edge lights tangent to M_1, the one on our left (or right) side is denoted as E_l (or E_r), respectively, where l means left (or r means right). A subregion of the FOI without any edge light cutting across is defined as a cell. As shown in Fig. 1, the rectangle where O locates, formed by four edge lights of sensors S_1 and S_4, is a cell. An edge light intersects with the boundary of the FOI or other edge lights generating intersections.

In an Euclidean plane, we define following concepts. If two edge lights intersect with each other at one intersection, they are intersecting; if they intersect with each other at more than one intersections, they are overlapping; if they have no intersection with each other, they are parallel. For the rest of this paper, the notations of variables are listed in Table I:

B. Problem Statement

In this paper, we study the MNC under multiple modulators by the following three aspects:

- First, the MNC is determined by the number of sensors (n) and the number of modulators ($m_i, i = 1 \ldots n$) to modulate each sensor. Given n and m_i, how to calculate the MNC is our first problem to study.
- Second, sometimes a deployment may not achieve the MNC. Under this condition, how to calculate the actual generated number of cells is our second problem to study.
- Third, the sufficient and necessary conditions to attain the MNC for a deployment is another problem to be studied. On one hand, when we design a deployment, we may need some rules to guide us so that we can design a deployment to achieve the MNC. On the other hand, if there is a deployment, we may need to judge whether it can achieve the MNC or not.

TABLE I
NOTATIONS

Notations	Descriptions
n	the number of sensors monitoring the FOI
m	the number of modulators modulating sensors
m_i or m_j	the number of modulators modulating the i-th sensor or the j-th sensor, $i, j = 1, 2, \ldots, n$
c	the number of cells in the FOI
$max(c)\|_{m,n}$	the maximum number of cells generated by n sensors and m modulators in the FOI
$max(c)\|_{n=1}$	when $n = 1$ sensors, the maximum number of cells segmented by edge lights in the FOI
$max(c)\|_{m_i=1}$	when $m_i = 1$ modulator modulates the i-th sensor, the maximum number of cells segmented by edge lights in the FOI
V_I	the number of intersections intersected by edge lights in the FOI
V_B	the number of intersections intersected by edge lights on the boundary of FOI (BFOI)
E_I	the number of edges generated by edge lights in the FOI
E_B	the number of edges intersected by edge lights with the BFOI
$max(\bullet)\|_k$	denotes the maximum number of $\bullet$ generated by k edge lights in the FOI.
$\Delta(\bullet)\|_k$	the differential between the maximum value and the actual value when there are k edge lights cutting across the FOI
k	the number of edge lights to segment the FOI
v	the number of edge lights intersecting with each other at one intersection in the FOI
V_e	the number of intersections each intersected by e edge lights in the FOI
W_w	the number of intersections each intersected by w edge lights on the BFOI
p	an intersection in the FOI
I	the number of intersections on one edge light
I_{max}	the maximum number of intersections on one edge light

III. Theories of the MNC and Relationships

In this section, first, we study the MNC with a given number of sensors and a given number of sensors modulators. Second, we study the scenarios in which deployments cannot achieve the MNC. Moreover, we provide a method to calculate the actual number of cells. Third, we study the sufficient and necessary conditions to achieve the MNC for any deployment.

A. Theorem of the MNC

In this part, we obtain Theorem 1 with a proof.

Theorem 1: If there are n sensors monitoring the FOI, each sensor is modulated by modulators m_i ($i = 1, \ldots, n$), and each

modulator only modulates one sensor, the MNC is given as follows:

$$c_{max} = \begin{cases} 2m_1 + 1, & n = 1 \\ \sum_{i=2}^{n}[2m_i(\sum_{j=1}^{i-1} 2m_j + 1)] + 2m_1 + 1, & n > 1 \end{cases} \quad (1)$$

As special cases, we have the following:

- if $m_i = m$ for any $i = 1, \ldots, n$, the equation $c_{max}|_{m_i=m} = 2m^2n^2 - 2m^2n + 2mn + 1$ holds;
- if $m_i = 1$ for any $i = 1, \ldots, n$, the equation $c_{max}|_{m_i=1} = 2n^2 + 1$ holds.

Proof: We prove the theorem with mathematical induction.

Firstly, if there is only one sensor and m_1 modulators to monitor the FOI, at most $2m_1$ edge lights cut through the FOI. These $2m_1$ edge lights do not intersect with each other in the FOI because they intersect at the location of the same sensor outside the FOI. The number of generated cells is at most $c_{max}|_{n=1} = 2m_1 + 1$.

Secondly, we prove the cases when $n > 1$. If $n = 2$, there are at most $2m_2 + 2m_1$ edge lights cutting across the FOI. In order to generate the MNC, each of the $2m_2$ edge lights of the second sensor should intersect with all the $2m_1$ edge lights of the first sensor. We can add such $2m_2$ one by one and calculate the number of cells. If one of the $2m_2$ edge lights intersects with the $2m_1$ edge lights, the FOI is segmented into at most $2(2m_1 + 1)$ cells. If two of the $2m_2$ edge lights intersect with the $2m_1$ edge lights, the FOI is segmented into at most $3(2m_1+1)$ cells. If all of the $2m_2$ edge lights intersect with the $2m_1$ edge lights, the FOI is segmented into at most $(2m_2 + 1)(2m_1 + 1)$ cells. Moreover, these $2m_2$ edge lights do not intersect with each other in the FOI. The number of generated cells is at most $c_{max}|_{n=2} = 2m_2(2m_1 + 1) + 2m_1 + 1 = \sum_{i=2}^{2}[2m_i(\sum_{j=1}^{i-1} 2m_j + 1)] + 2m_1 + 1$. Hence, if $n = 2$, the equation holds.

If $n = k$, we assume that $c_{max}|_{n=k} = \sum_{i=2}^{k}[2m_i(\sum_{j=1}^{i-1} 2m_j + 1)] + 2m_1 + 1$ holds. Then, for $n = k + 1$, the $(k + 1)$-th sensor has m_{k+1} modulators and generates at most $2m_{k+1}$ edge lights. If each of the edge lights cuts through all the edge lights, which are not belonging to the $(k+1)_{th}$ sensor, at most other $2m_{k+1}(\sum_{j=1}^{i-1} 2m_j + 1)$ cells are generated. Then, we have $c_{max}|_{n=k+1} = 2m_{k+1}(\sum_{j=1}^{i-1} 2m_j + 1) + c_k = \sum_{i=2}^{k+1}[2m_i(\sum_{j=1}^{i-1} 2m_j + 1)] + 2m_1 + 1$. Hence, the equation holds for $n > 1$.

If $m_i = m$ for any $i = 1, \ldots, n$, we have $c_{max}|_{m_i=m} = \sum_{i=2}^{n}[2m(\sum_{j=1}^{i-1} 2m + 1)] + 2m + 1 = 4m^2 \sum_{i=2}^{n}(i - 1) + 2m(n - 1) + 2m + 1 = 2m^2n^2 - 2m^2n + 2mn + 1$.

If $m_i = 1$ for any $i = 1, \ldots, n$, we have $c_{max}|_{m_i=1} = \sum_{i=2}^{n}[2(\sum_{j=1}^{i-1} 2 + 1)] + 2 + 1 = 2n^2 + 1$. Hence, theorem 1 holds. ■

B. Relationships of Intersections, Edges, and Cells

To study the relationship between the number of intersections and the number of cells in the FOI, we will apply Euler's Formula $V + F - E = 2$ [27], defined based on a connected plane graph G constructed by the FOI with V vertices, E edges, and F faces. In this paper, we discuss graphs or subgraphs in the 2-dimensional plane with more than one vertex and more than one edge. By not counting the region outside the FOI, we have $V + F - E = 1$ [25]. Let V_b and E_b denote the number of intersections and the number of edges on the boundary of the FOI, respectively. Let V_I and E_I denote the number of intersections and the number of edges in the FOI, respectively. Therefore, we have $V = V_I + V_b$, $E = E_I + E_b$, and $F = c$. Then, we have the following theorem.

Theorem 2: Euler's Formula can be applied to the graph G which is constructed by the FOI and edge lights. By not counting the region outside the FOI, Euler's formula for the graph G has the following form

$$V_I + V_b - E_e - E_b + c = 1. \quad (2)$$

Moreover, this equation can be simplified as

$$V_I - E_e + c = 1. \quad (3)$$

Proof: First, the authors in [27] prove that the numbers of vertices, edges, and faces of a finite graph G satisfy $V + F - E = 2$ whenever the graph is or can be drawn on the plane. Thus, the graphs on the FOI can be applied to Euler's Formula by satisfying the following two conditions: a) the FOI and edge lights can be drawn in the same 2-dimensional plane; b) the graphs on the FOI are finite graphs. Although the sensors and modulators are 3-dimensional objects in a 3-dimensional space, as illustrated in Fig. 1, edge lights and the FOI can be drawn on a 2-dimensional plane that parallels to the floor or the horizontal plane. Moreover, the maximum number of cells can be calculated with theorem 1, indicating that the edges, vertices, and faces of the graphs on the FOI are finite and the graphs are also finite. Hence, the Euler's Formula can be applied to the graph G in the FOI: by not counting the region outside of the FOI, we have $V + F - E = 1$.

Second, since we have $V = V_I + V_b$, $E = E_I + E_b$, and $F = c$, we plug them into the above equation and we have equation (2).

Third, we try to simplify equation (2). A graph G_b is constructed with V_b vertices, E_b edges, and F_b faces, and the whole region of the FOI is assumed to be a face, i.e., $F_b = 1$. Thus, we have $G_b \subseteq G$, i.e., G_b is an induced subgraph of G, indicating that all of the vertices, edges, and faces of graph G_b also belong to graph G [28]. In other words, graph G_b also satisfies the two conditions a) and b) in the first part of this proof. Thus, we can employ Euler's Formula on G_b as well. Based on the Euler's Formula and not counting the region outside the FOI, we have $V_b + F_b - E_b = 1$, i.e., $V_b - E_b = 0$. Then, the equation (2) is simplified as $V_I + c - E_e = 1$. ■

There are three kinds of intersection locations for edge lights: in the FOI, out the FOI, and on the boundary of the FOI. For edge lights, if two of them generate an intersection in the

outside of the FOI, this intersection has no contribution to the segmentation of the FOI; if an edge light cuts across the FOI, the edge light generates two intersections on the boundary of the FOI and segments the FOI into cells; if two edge lights intersect with each other in the FOI on a 2-dimensional plane, the following results can be obtained:

- These two edge lights cut across the FOI and each of them generates two intersections on the boundary of the FOI;
- The four intersections on the boundary of the FOI do not overlap with each other.
- The generated intersection in the FOI 'segments' the FOI with one more cell than the case without an intersection. This can be verified by Lemma 1.

Next, we utilize Euler's Formula to further study relationships among intersections, edges, and cells.

Lemma 1: When no edge lights cut across the FOI, the whole FOI is a cell. If k ($k > 0$) edge lights cut across the FOI, the relationships between intersections and cells are described as follows:

- ***Relationship 1***: If these k edge lights intersect with the boundary of the FOI with $2k$ different intersections, the number of cells in the FOI increases k than that when no edge lights cut across the FOI.
- ***Relationship 2***: If these k edge lights intersect with each other in the FOI at V_I ($V_I > 0$) different intersections in the FOI and each intersection is only intersected by two edge lights, there are V_I more cell in the FOI than the case that none of those k edge lights intersecting with each other in the FOI.

Proof: We prove *Relationship 1* as follows. When $V_I = 0$, k ($k \geq 1$) edge lights cut across the FOI intersecting no intersections in the FOI, and we have $E_e \neq 0$. Based on equation (3), we have $c - E_e = 1$. Since all of the edge lights cut across the FOI, each of them intersects with the boundary of the FOI with two intersections and generates an edge in the FOI. We have $E_e = k$ and $c = k + 1$. In other words, these k edge lights or these $2k$ intersections on the boundary of the FOI generate k additional cells. Hence, *Relationship 1* holds when $V_I = 0$. For the case $V_I > 0$, we will continue to prove *Relationship 1* after *Relationship 2* is approved.

We prove *Relationship 2* as follows. We adopt mathematical induction. If there are intersections in the FOI (i.e., $V_I > 0$), the number of edge lights should satisfy $k \geq 2$ since at least two edge lights generate an intersection. If k ($k \geq 2$) edge lights cut across the FOI and only two of the k edge lights intersect at an intersection in the FOI (i.e., $V_I = 1$), this intersection divides the each of the two edge lights in the FOI into two edges so that the number of edges increases by two. Since $E_e|_{V_I=0} = k$ has been proved, we have $E_e|_{V_I=1} = k + 2$. Plugging this in equation (3), we have $1 + c|_{V_I=1} - (k + 2) = 1$, i.e., $c|_{V_I=1} = (k + 1) + 1 = k + 2$. If there are $V_I = p$ intersections in the FOI and each intersection only intersected by two edge lights, we assume $c|_{V_I=p} = (k + 1) + p$. Based on equation (3), we have $E_e|_{V_I=p} = c|_{V_I=p} + p - 1 = (k + 1) + p + p - 1 = 2p + k$.

Then, if there are $V_I = p + 1$ intersections and each is intersected by only two edge lights, there is one more intersection in the FOI than that of $V_I = p$. This additional intersection generates two additional edges, i.e., $E_e|_{V_I=p+1} = E_e|_{V_I=p} + 2 = 2p + k + 2$. By substituting $V_I = p + 1$ and $E_e|_{V_I=p+1} = 2p + k + 2$ into equation (3), we have $p + 1 - (2p + k + 2) + c|_{V_I=p+1} = 1$, i.e., $c|_{V_I=p+1} = (k + 1) + (p + 1)$. Hence, the second relationship holds.

We will continue to prove *Relationship 1* next. We will prove that the number of intersections V_I does not influence the number of cells generated by those k edge lights intersecting on the boundary of the FOI. When V_I increases from 0 to p in the above, the values of c can be expressed as: $c|_{V_I=0} = (k + 1) + 0, c|_{V_I=1} = (k + 1) + 1, \ldots, c|_{V_I=p} = (k + 1) + p$. In those equations of c, there is a $(k + 1)$ for each equation, which is not influenced by the values of V_I. From the proof of the first relationship when $V_I = 0$ in the above, the "k" corresponds to the number of cells generated by k edge lights intersecting the boundary of the FOI, and the "1" corresponds to the whole FOI when no edge lights cut across the FOI. Hence, no matter what the value of V_I is, they're still k cells generated by those k edge lights intersecting on the boundary of the FOI. In other words, the intersections in the FOI do not eliminate those $k + 1$ cells but geometrically make a further segmentation of the FOI. Hence, the first relationship holds. Hence, lemma 1 holds. ■

Notice that when two edge lights are tangent with the boundary of the FOI at two different intersections, these two intersections do not generate any cell in the FOI due to no edge lights cutting across the FOI.

To generate the maximum number of intersections in the FOI, each of the k edge lights must intersect with each other in the FOI. There is a problem that multiple edge lights intersect at the same intersection so that intuitively, the maximum number of intersections cannot be achieved. Since two edge lights can only intersect with each other once in the FOI on a 2-dimensional plane, when multiple edge lights intersect at one intersection in the FOI, the number of intersections is decreased. For example, three edge lights intersecting with each other can generate three intersections, but only one intersection is generated when they intersect at one intersection. Hence, for edge lights to generate the maximum number of intersections in the FOI, we define the following **INTE (Intersection) conditions**:

$$\textit{INTE-conditions} = U_1 \wedge U_2, \tag{4}$$

where U_1={all k edge lights intersect with each other in the FOI} and U_2={each intersection is just intersected by two edge lights}.

If the INTE conditions are not satisfied, multiple edge lights may intersect at one intersection in the FOI or some edge lights do not intersect at all. Based on DeMorgan's Law, **the reverse of INTE conditions** is:

$$\overline{INTE - conditions} = \overline{U_1 \wedge U_2} = \overline{U_1} \vee \overline{U_2}, \tag{5}$$

where $\overline{U_1}$={at least two of the k edge lights do not intersect in the FOI} and $\overline{U_2}$={at least one intersection is intersected by more than two edge lights in the FOI}.

We can calculate V_I differently from Theorem 2 as follows:

$$V_I = \sum_{e=2}^{k} V_e, \tag{6}$$

where k denotes the number of edge lights and V_e denotes the number of intersections intersected by exact e edge lights. For instance, $v_3 = 4$ means that there are exact 4 intersections in the FOI and each is intersected by 3 edge lights. Moreover, if the INTE conditions are satisfied, we have $V_e|_{e=2} \neq 0$ and $V_e|_{e>2} = 0$.

Lemma 2: The maximum number of intersections in the FOI can be achieved by k ($k \geq 2$) edge lights is

$$max(V_I)|_k = k(k-1)/2. \tag{7}$$

Then, the INTE conditions are satisfied.

Proof: There are at most $k-1$ intersections on each edge light and there are total k edge lights. Since two edge lights intersect at one intersection, the total number of interactions should be divided by 2. Therefore, the maximum number of intersections is $k(k-1)/2$.

We prove that the INTE conditions should be satisfied when the maximum number of intersections in the FOI is achieved by k edge lights. We compare the number of intersections generated by k edge lights satisfying the $\overline{U_1}$ or $\overline{U_2}$ condition with that satisfying the INTE conditions, respectively. When k edge lights satisfying the INTE conditions, there are $k-1$ intersections on each edge light in the FOI due to the definition of the INTE conditions, and $k-1$ is the maximum number of intersections on an edge light. When k edge lights satisfying the $\overline{U_1}$ condition, suppose that E_i and E_{i+1} are the two edge lights that do not intersect with each other in the FOI. Then, we have $I_i < k-1$, where I_i is the number of intersections on the edge light E_i. When k edge lights satisfying the $\overline{U_2}$ condition, suppose that E_j, E_{j+1}, and E_{j+2} are the three edge lights that intersect at one intersection in the FOI. Then, we have $I_j < k-1$, where I_j is the number of intersections on the edge light E_j. Hence, the number of intersections in the FOI under the $\overline{U_1}$ or $\overline{U_2}$ condition is less than that under the INTE conditions. Hence, the INTE conditions are satisfied when the maximum number of intersections is achieved by k edge lights. Hence, lemma 2 holds. ■

Lemma 3: If k ($k \geq 2$) edge lights cut across the FOI, the number of edges in the FOI can be calculated as:

$$E_I = k + \sum_{e=2}^{k} eV_e, \tag{8}$$

where V_e denotes the number of intersections intersected by e edge lights.

Proof: Since k edge lights cut across the FOI, each must cut across the FOI and generate two intersections with the boundary of FOI (BFOI). Since these two intersections segment one edge for each edge light, totally k edges are formed from the k edge lights. Moreover, any other intersections in the FOI on this edge light must sit between these two intersections. Any intersection between these two intersections divides the edge E into two edges and therefore generates one additional edge. If e edge lights intersect with each other at one intersection, there is one additional edge generated on each of those e edges lights, i.e., total e additional edges for e edge lights. Therefore there are eV_e additional edges generated by those V_e intersections. Hence, lemma 3 holds. ■

Lemma 4: The maximum number of edges in the FOI generated by k edge lights is

$$max(E_I)|_k = k^2 \tag{9}$$

Proof: We prove lemma 4 with mathematical induction.

If $k = 2$, we can easily see that $max(E_I)|_{k=2} = 4$ holds.

Assume that if $k = q$, $max(E_I)|_q = q^2$ holds. Then, there are q^2 edges in the FOI. If $k = q+1$, to generates the maximum number of edges, the $(q+1)$-th edge light intersects with other q edge lights and generates one additional intersection on each of the q edge lights. Then, each of the q edge lights has an additional edge, i.e., total q additional edges. Since the $(q+1)$-th edge light must cut across the BFOI and generate two intersections on the BFOI, there are q intersections in the FOI and 2 intersections on the BFOI so that they forms $(q+1)$ edges for the $(q+1)$-th edge light. There are a total $q^2+q+q+1 = (q+1)^2$ edges in the FOI. Hence, lemma 4 holds with $k = q+1$. ■

In fact, the proof of lemma 4 implies that one intersection in the FOI on an edge light makes the edge light one additional edge.

Lemma 5: If k ($k \geq 2$) edge lights cut across the FOI, the number of cells generated by k edge lights is

$$c = k + \sum_{e=2}^{k} (e-1)V_e + 1. \tag{10}$$

Proof: Based on theorem 2, we have $c = E_I - V_I + 1$. By plugging equation (8) and equation (6) into $c = E_I - V_I + 1$ and simplifying the result, we prove the lemma. ■

Lemma 6: If k ($k \geq 2$) edge lights cut across in the FOI, they segment the FOI into at most $k(k+1)/2+1$ cells, i.e.,

$$\max(c)|_k = k(k+1)/2 + 1, \tag{11}$$

Then, the INTE conditions are satisfied.

Proof:

First, we prove lemma 6 with mathematical induction under INTE conditions. It is easy to know that the presence order of edge lights does not affect the segmentation result of the FOI. We segment the FOI by adding one edge light each time and ensure that each edge light intersects with all the other edge lights. When $n = 2$, two edge lights are intersecting with each other and segmenting the FOI into $2(2+1)/2+1 = 4$ cells. When $n = k$, we assume that the FOI is segmented into $k(k+1)/2+1$ cells holds. When $n = k+1$, the $(k+1)$-th edge light intersects with all the other edge lights and generates $k+1$ new cells. There are total $k(k+1)/2+1+k+1 = (k+1)(k+2)/2+1$ cells.

Second, we prove lemma 6 if INTE conditions are not satisfied, i.e., either $\overline{U_1}$ or $\overline{U_2}$ satisfies. If condition $\overline{U_1}$ is satisfied, at least two of the k edge lights have no intersection with each other in the FOI. We denote such edge lights pairs with $E_p = \{(E_i, E_j), \dots\}$ $(i, j \in \{1, 2, \dots, k\},\ i < j)$, and denote the number of such pairs with $|E_p|$ ($|E_p| \in \{1, 2, \dots\}$). Based on the definition of the INTE conditions and

no intersections generated by $|E_p|$ pairs of edge lights under the $\overline{U_1}$ condition, we obtain $V_I|_{INTE} - V_I|_{\overline{U_1}} \geq |E_p|$, where $V_I|_{INTE}$ and $V_I|_{\overline{U_1}}$ are the number of intersections in the FOI under the INTE conditions and the $\overline{U_1}$ condition, respectively. Moreover, $V_I|_{INTE} - V_I|_{\overline{U_1}} = |E_p|$ is only achieved when each of the intersection in the FOI was intersected by only two edge lights under the $\overline{U_1}$ condition. When there exists an intersection intersected by more than two edge lights under the $\overline{U_1}$ condition, we have $V_I|_{INTE} - V_I|_{\overline{U_1}} > |E_p|$. There are at least $|E_p|$ more intersections under the INTE conditions than under the $\overline{U_1}$ condition. Based on lemma 1, the edge lights under the $\overline{U_1}$ condition generate at least E_p fewer cells than the case under the INTE conditions. If condition $\overline{U_2}$ is satisfied, at least one intersection is intersected by more than two edge lights in the FOI. We denote the number of such intersections with V_e ($V_e \in \{1, 2, \dots\}$) and $\exists e, e \geq 3 \wedge V_e > 0$. Now, we consider the number of cells generated by these e edge lights. We apply equation (3) to the intersections, edges, and cells generated by the e edge lights, i.e., $V_I|_e - E_I|_e + c|_e = 1$. Since there is one intersection, we have $V_I|_e = 1$. Moreover, each edge generates two edges by intersecting at this intersection. There are e edge lights generating $2e$ edges. Then, we have $1-2e+c|_e = 1$, i.e., $c|_e = 2e$. The e edge lights segment the FOI into $2e$ cells. On the other hand, we know that e edge lights segment the FOI into $e(e+1)/2+1$ cells under the INTE conditions. By utilizing the number of cells generated by e edge lights under condition $\overline{U_2}$ to subtract the number of cells generated by e edge lights under INTE conditions, we obtain $2e - (e(e+1)/2 + 1) = -(e-2)(e-1)/2 < 0$ for any $e \in \{3, 4, \dots, k\}$. It is obvious that condition $\overline{U_2}$ cannot achieve the maximum number of cells. Hence, the maximum number of cells can only be achieved under the INTE conditions, i.e, $max(c)|_k = k(k+1)/2 + 1$. Hence, lemma 6 holds. ■

We define a differential operator, denoted as $\Delta(\bullet)|_k$, to measure the difference between the maximum value of $\bullet$ and the actual generated $\bullet$ in the FOI,

$$\Delta(\bullet)|_k = max(\bullet)|_k - \bullet, \tag{12}$$

where the $\bullet$ can be replaced by V_I, E_I, or c generated by k edge lights cutting across the FOI, respectively. We obtain intersection differential, edge differential, and cell differential denoted as $\Delta(V_I)|_k$, $\Delta(E_I)|_k$, $\Delta(c)|_k$, respectively.

Lemma 7: If k ($k \geq 2$) edge lights cut across in the FOI, we have

$$\Delta(V_I)|_k = max(V_I)|_k - V_I = k(k-1)/2 - \sum_{e=2}^{k} V_e, \tag{13}$$

$$\Delta(E_I)|_k = max(E_I)|_k - E_I = k^2 - k - \sum_{e=2}^{k} eV_e, \tag{14}$$

$$\Delta(c)|_k = max(c)|_k - c = k(k-1)/2 - \sum_{e=2}^{k} (e-1)V_e, \tag{15}$$

where $\Delta(V_I)|_k$, $\Delta(E_I)|_k$ and $\Delta(c)|_k$ denote the intersection differential, the edge differential, and the cell differential, respectively.

Proof: For the intersection differential, based on the definition of intersection differential we have $\Delta(V_I)|_k = max(V_I)|_k - V_I$. Then, based on equation (6) and lemma 2, we obtain $\Delta(V_I)|_k = k(k-1)/2 - \sum_{e=2}^{k} V_e$.

For the edge differential, based on the definition of edge differential, we have $\Delta(E_I)|_k = max(E_I)|_k - E_I$. Then, based on lemma 3 and lemma 4, we obtain $\Delta(E_I)|_k = k^2 - k - \sum_{e=2}^{k} eV_e$.

For the cell differential, based on the definition of cell differential, we have $\Delta(c)|_k = max(c)|_k - c$. Then, based on equation (10) and lemma 6, we obtain $\Delta(c)|_k = k(k-1)/2 - \sum_{e=2}^{k} (e-1)V_e$. Hence, lemma 7 holds. ■

Lemma 8: When k edge lights cut cross in the FOI, the intersection differential, the edge differential, and the cell differential satisfy the following equation:

$$\Delta(V_I)|_k - \Delta(E_I)|_k + \Delta(c)|_k = 0. \tag{16}$$

Proof: Plugging equations (13), (14), and (15) into equation (16), we have

$$k(k-1)/2 - \sum_{e=2}^{k} V_e - (k^2 - k - \sum_{e=2}^{k} eV_e) + k(k-1)/2 - \sum_{e=2}^{k} (e-1)V_e = 0$$

Hence, lemma 8 holds. ■

Theorem 3: When k edge lights cut across the FOI, we have:

- If one of V_I, E_I and c achieves the maximum value, the other two achieve their maximum values as well;
- The maximum values of V_I, E_I and c satisfy the Euler's Formula, i.e.,

$$max(V_I)|_k - max(E_I)|_k + max(c)|_k = 1. \tag{17}$$

Proof: For the first conclusion, we first prove two special cases $k = 0$ and $k = 1$, and then prove the case $k \geq 2$ by contradictions.

When $k = 0$, there is no edge light cutting across the FOI. We can obtain $V_I = max(V_I)|_k = 0$, $E_I = max(E_I)|_k = 0$, and $c = max(c)|_k = 1$. In other words, all of V_I, E_I and c achieve their maximum values.

When $k = 1$, there is one edge light cutting across the FOI. We can obtain $V_I = max(V_I)|_k = 0$, $E_I = max(E_I)|_k = 1$, and $c = max(c)|_k = 2$. Since the edge light cuts across the FOI, all of V_I, E_I and c achieve their maximum values.

When $k \geq 2$, the first conclusion is classified into three cases: I, II, III. We prove three cases with contradictions.

Case I: When $V_I = max(V_I)|_k$, we prove $E_I = max(E_I)|_k$ and $c = max(c)|_k$. Base on lemma 2, we obtain that the INTE conditions are satisfied when $V_I = max(V_I)|_k$. Since each intersection is intersected by two edge lights under the INTE conditions, we have $V_2 = 0$ and $V_e = 0$ when $e \in \{3, 4, \dots, k\}$. Based on equation (13), we have $\Delta(V_I)|_k = 0$ and $\sum_{e=2}^{k} V_e = V_2 = k(k-1)/2$. Plugging the above into equation (14) and equation (15), we obtain $\Delta(E_I)|_k = 0$ and $\Delta(c)|_k = 0$, respectively. Plugging $\Delta(E_I)|_k = 0$ and

$\Delta(c)|_k = 0$ into equation (14) and equation (15), we obtain $E_I = max(E_I)|_k$ and $c = max(c)|_k$, respectively. Hence, Case I holds.

Case II: When $E_I = max(E_I)|_k$, we prove $V_I = max(V_I)|_k$ and $c = max(c)|_k$ with contradictions. Under $E_I = max(E_I)|_k$, we define the following equations:

$$A_0 = \{V_I = max(V_I)|_k \wedge\ c = max(c)|_k\},$$
$$A_1 = \{V_I \neq max(V_I)|_k \wedge\ c \neq max(c)|_k\},$$
$$A_2 = \{V_I \neq max(V_I)|_k \wedge\ c = max(c)|_k\},$$
$$A_3 = \{V_I = max(V_I)|_k \wedge\ c \neq max(c)|_k\}.$$

Then, we have $\overline{A_0} = A_1 \vee A_2 \vee A_3$. Now, we prove that A_1, A_2, and A_3 do not hold, respectively.

First, suppose that A_1 holds under $E_I = max(E_I)|_k$. Since $V_I \neq max(V_I)|_k$ and $c \neq max(c)|_k$, we obtain $\Delta(V_I)|_k \neq 0$ and $\Delta(c)|_k \neq 0$. Moreover, based on the definition of differential operators, we know $\Delta(V_I)|_k > 0$ and $\Delta(c)|_k > 0$. Hence, $\Delta(V_I)|_k + \Delta(c)|_k > 0$. Base on equation (16), we obtain $\Delta(V_I)|_k + \Delta(c)|_k = \Delta(E_I)|_k$. Then, we have $\Delta(E_I)|_k > 0$. However, based on equation (14), we obtain $\Delta(E_I)|_k = max(E_I)|_k - E_I = 0$ when $E_I = max(E_I)|_k$. Then, this is contradiction. Hence, A_1 does not hold under $E_I = max(E_I)|_k$.

Second, suppose that A_2 holds under $E_I = max(E_I)|_k$. Since A_2 holds, we obtain $c = max(c)|_k$. Plugging $E_I = max(E_I)|_k$ and $c = max(c)|_k$ into equation (14) and equation (15), we obtain $\Delta(E_I)|_k = \Delta(c)|_k = 0$. Plugging $\Delta(E_I)|_k = \Delta(c)|_k = 0$ into equation (16), we obtain $\Delta(V_I)|_k = 0$. Then, we plug $\Delta(V_I)|_k = 0$ into equation (13) and obtain $V_I = max(V_I)|_k$. That is in contradiction with $V_I \neq max(V_I)|_k$ in A_2. Hence, A_2 does not hold under $E_I = max(E_I)|_k$.

Third, suppose that A_3 holds under $E_I = max(E_I)|_k$. Since A_3 holds, we obtain $V_I = max(V_I)|_k$. Plugging $E_I = max(E_I)|_k$ and $V_I = max(V_I)|_k$ into equation (13) and equation (14), we obtain $\Delta(V_I)|_k = \Delta(E_I)|_k = 0$. Plugging $\Delta(V_I)|_k = \Delta(E_I)|_k = 0$ into equation (16), we obtain $\Delta(c)|_k = 0$. Then, we plug $\Delta(c)|_k = 0$ into equation (15) and obtain $c = max(c)|_k$. That is in contradiction with $c \neq max(c)|_k$ in A_3. Hence, A_3 does not hold under $E_I = max(E_I)|_k$. Hence, under $E_I = max(E_I)|_k$, A_0 holds and Case II holds.

Case III: When $c = max(c)|_k$, we prove $V_I = max(V_I)|_k$ and $E_I = max(E_I)|_k$. Based on the lemma 6, we know that the INTE conditions should be satisfied when $c = max(c)|_k$. Under the INTE conditions, the maximum number of intersections is achieved, i.e., $V_I = max(V_I)|_k$. Plugging $V_I = max(V_I)|_k$ and $c = max(c)|_k$ into equation (13) and equation (15), respectively, we obtain $\Delta(V_I)|_k = \Delta(c)|_k = 0$. Then, plugging $\Delta(V_I)|_k = \Delta(c)|_k = 0$ into equation (16), we obtain $\Delta(E_I)|_k = 0$. By plugging $\Delta(E_I)|_k = 0$ into equation (15), we obtain $E_I = max(E_I)|_k$. Hence, Case III holds. Hence, the first conclusion holds.

Now, we prove the second conclusion. Since $V_I = max(V_I)|_k$, $E_I = max(E_I)|_k$ and $c = max(c)|_k$, we prove that $max(V_I)|_k$, $max(E_I)|_k$ and $max(c)|_k$ satisfy the Euler's Formula, i.e., equation (3). Adding the left side and the right side of equation (16) with the left side and the right side of equation (3), respectively, we obtain $V_I + \Delta(V_I)|_k - \Delta(E_I)|_k - E_I + \Delta(c)|_k + c = 1$. Then, plugging equation (13), equation (14), and equation (15) into the above equation, we obtain equation (17). Hence, the second conclusion holds and theorem 3 holds. ■

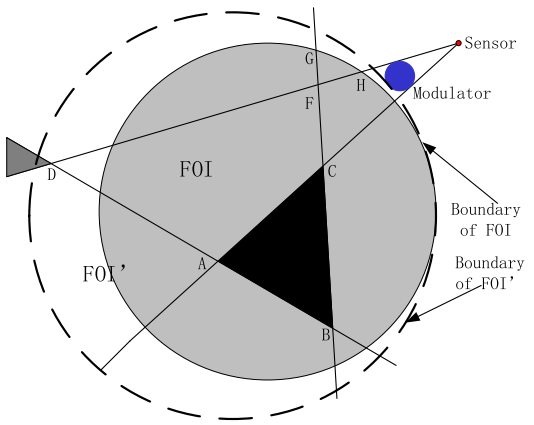

Fig. 2. The example to illustrate concept degenerated cells.

C. Calculation of the Actual Number of Cells

We introduce a definition as 'degenerated' cells. For instance, assume that there are three edge lights. Any two of the three edge lights intersect at an intersection. As illustrated in Fig. 2, such three edge lights AC, AB, and BC construct a triangle cell ABC with three intersections A, B, and C as its vertices. If these three edge lights intersect at the same intersection (namely, A, B, and C overlap with each other), the triangle cell cannot be generated (or we can say the triangle ABC is 'degenerated'). Accordingly, we define the 'degenerated' cells as follows.

Definition 1: If one of the three following cases happens, there is one cell that cannot be generated in the FOI. We claim that the cell is degenerated.

- Case I, three or more edge lights intersect at the same intersection;
- Case II, two edge lights of different sensors intersect outside the FOI;
- Case III, two edge lights intersect at the same intersection on the boundary of the FOI.

Next, we explain the reasons why the cell is degenerated in case II and case III. First, if the intersection of two edge lights is outside the FOI, there is one cell fewer than that of the intersection inside the FOI. For example, the grey region with a vertex as D is outside the FOI and inside the FOI'. We can observe that the grey region generates a cell with a vertex as D inside the FOI', but the cell is outside the FOI. Hence, we claim that this grey cell is degenerated. Second, if the intersection of two edge lights is on the boundary of the FOI, there will be one cell fewer than that of the intersection inside the FOI. For example, if the intersection F on the boundary of the FOI, the cell GFH will not be inside the FOI. Then, we say the cell GFH is degenerated. Accordingly, we provide three lemmas to calculate the number of degenerated cells.

Lemma 9: If an edge light intersects with u edge lights of other sensors generating k intersections outside the FOI, there are k cells degenerated.

Proof: According to the definition of edge light, an edge light should cut across the FOI. As illustrated in Fig. 2, an edge light always constructs cells with other edge lights or the boundary of FOI. Assume that the region inside the dots line circle is the FOI'. It is easy to know that the intersection D is inside FOI' but outside the FOI. Compare the cells inside the FOI with the cells inside the FOI', we can find that the grey cell with a vertex D is outside the FOI, and the other cells are inside the FOI or part of them inside the FOI. For the part of the cell inside the FOI, it is easy to know they change their edge on the boundary of the FOI' into the edge on the boundary of the FOI. Similarly, if an edge light intersects with other k edge lights outside the FOI, there are k cells outside the FOI and these $u+1$ edge lights construct cells with the boundary of the FOI. Hence, lemma 9 holds. ■

Lemma 10: k ($k \geq 2$) edge lights intersecting at an intersection in the FOI generate $2k$ cells. k ($k \geq 2$) edge lights intersecting at an intersection on the BFOI generate $k+1$ cells in the FOI.

Proof: Denote the intersection as P. When P is in the FOI, we prove this lemma with mathematical induction. When $k=2$, there are two edge lights intersecting at P and segmenting the FOI into $2k=4$ cells. When $k=e$, assume that the FOI is segmented into $2e$ cells by e edge lights intersecting at P. When $k=e+1$, the $(e+1)$-th edge light E_{e+1} intersects with all the other edge lights at P. There exist i, j $(1 \leq i, j \leq e)$ such that E_{e+1} is the only edge light between E_i and E_j. All of E_i, E_j, and E_{e+1} pass through P. Before E_{e+1} passes through P, there are two cells between E_i and E_j. When E_{e+1} cuts across the FOI and passes through P, E_{e+1} segments the two cells between E_i and E_j into four cells. Then, there are $2e+2=2(e+1)$ cells in the FOI.

When P is on the BFOI, the subregions outside the FOI are not cells. Since all the k edge lights pass through P, the number of cells is clearly $k+1$. Hence, lemma 10 holds. ■

Lemma 11: For k ($k \geq 2$) edge lights intersecting at an intersection P in the FOI, the number of the degenerated cells generated by these k edge lights is $(k-2)(k-1)/2$.

Proof: Based on lemma 6, k edge lights can at most generate $k(k+1)/2+1$ cells in the FOI. Based on lemma 10, k edge light intersecting at P in the FOI can generate $2k$ cells. Then, there are $k(k+1)/2+1-2k=(k-2)(k-1)/2$ cells degenerated. Hence, lemma 11 holds. ■

Lemma 12: For k ($k \geq 2$) edge lights intersecting at an intersection P on the BFOI, the number of degenerated cells is $k(k-1)/2$.

Proof: Based on lemma 6, k edge lights can at most generate $k(k+1)/2+1$ cells in the FOI. Based on lemma 10, k edge light intersecting at P on the BFOI can generate $k+1$ cells. Then, there are $k(k+1)/2+1-(k+1)=k(k-1)/2$ cells degenerated. Hence, lemma 12 holds. ■

First, we discuss the intersections (such as D in Fig. 2) outside the FOI with lemma 9, indicating that some cells are generated outside the FOI. According to [23], the authors assert that under the condition $n>1$, adding one intersection means adding one cell. On the contrary, decreasing one intersection means decreasing one cell in the FOI.

Second, we discuss the overlapping intersections in the FOI with lemma 11 or on the boundary of the FOI with lemma 12. In other words, if more than two edge lights intersect at the same intersection, more than one cell is degenerated.

Theorem 4: In a deployment of sensors and modulators, given the values of I_{ij}, I'_{ij}, B_{ij}, B'_{ij}, e, V_e, h, w, W_w, and g, where

- I_{ij} and I'_{ij} denote the number of intersections on the left edge light El_{ij} and right edge light Er_{ij} in the FOI, respectively; i and j denote the i-th sensor and its j-th modulator, respectively;
- B_{ij} and B'_{ij} denote the number of intersections on the boundary of the FOI of the left and right edge lights (namely, El_{ij} and Er_{ij}), respectively;
- for an intersection in the FOI, e denotes the number of edge lights intersecting at this intersection, V_e denotes the number of intersections intersected by e edge lights, and h denotes the maximum value of e;
- for an intersection on the boundary of the FOI, w denotes the number of edge lights intersecting at this intersection, W_w denotes the number of intersections intersected by w edge lights, and g denotes the maximum value of w,

the number of cells obtained by the deployment is:

$$c = c_{max} - con_1 - con_2 - con_3,$$

where $con_1 = \sum_{i=1}^{n}(2m_i + 2 - B_{ij} - B'_{ij} - \sum_{j=1}^{m_j}\frac{(I_{ij}+I'_{ij})}{2})$, $con_2 = \sum_{e=3}^{h}\frac{V_e(e-2)(e-1}{)}2$, and $con_3 = \sum_{w=2}^{g}\frac{W_w(w-1)w}{2}$.

Proof: We prove this theorem by analyzing the three cases in lemma 9, lemma 11, and lemma 12. If the case in lemma 9 happens, there are $con_1 = \sum_{i=1}^{n}(2m_i + 2 - B_{ij} - B'_{ij} - \sum_{j=1}^{m_j}\frac{(I_{ij}+I'_{ij})}{2})$ number of cells degenerated. If the case in lemma 11 happens, there are $con_2 = \sum_{e=3}^{h}\frac{V_e(e-2)(e-1}{)}2$ number of cells degenerated. If the case in lemma 12 happens, there are $con_3 = \sum_{w=2}^{g}\frac{W_w(w-1)w}{2}$ number of cells degenerated. Utilizing c_{max} deducted by the number of the degenerated cells, we have the number of actual obtained cells: $c = c_{max} - con_1 - con_2 - con_3$. ■

Theorem 4 can be utilized to calculate the number of cells in a deployment algorithm that may not achieve the MNC. The difference between theorem 1 and theorem 4 is that theorem 1 only needs to know the number of sensors and modulators to be deployed, and theorem 4 should also know the number of intersections on each edge lights in a given deployment of sensors and modulators.

D. Sufficient and Necessary Conditions of the MNC

In a Euclidean plane, there are three kinds of relationships between two lines: intersecting, overlapping, and parallelling. If two edge lights overlap with each other, they are the same

edge light. If two edge lights parallel with each other, they can construct at most three cells with the boundary line of the FOI. If a deployment generates the MNC, every two edge lights must intersect with each other. Under this condition, we discuss the intersection relationship among edge lights.

Theorem 5: An algorithm can achieve the MNC, if and only if it satisfies three conditions:

- each edge light should intersect with all the other edge lights in the FOI except those originating from the same sensor;
- there should be no more than two edge lights intersecting on the same intersection in the FOI;
- there should be no more than one edge light intersecting on the same intersection on the boundary of the FOI.

Proof: We prove theorem 5 in its sufficient and necessary property.

For the sufficient property, if an algorithm satisfies the three conditions in theorem 5, there are no cells degenerated. According to theorem 4, we have $c = c_{max}$. Hence, the sufficient property holds.

For the necessary property, we prove theorem 5 by contradictions. Suppose that an algorithm cannot obtain the MNC. According to theorem 4, at least one of the three equations $con_1 \neq 0$, $con_2 \neq 0$, and $con_3 \neq 0$ hold. If $con_1 \neq 0$ holds, the first condition in theorem 5 cannot be satisfied. If $con_2 \neq 0$ holds, the second condition in theorem 5 cannot be satisfied. If $con_3 \neq 0$ holds, the third condition in theorem 5 cannot be satisfied. These contradict with that all the three conditions are satisfied. Hence, the necessary property holds.

Hence, theorem 5 holds. ■

In fact, lemma 9, lemma 11, and lemma 12 provide three scenarios that the MNC cannot be achieved. Based on the three lemmas, we provide two theorems (theorem 5 and theorem 6) as the necessary and sufficient conditions to achieve the MNC. These two theorems can be utilized to design an algorithm or judge whether an algorithm generating the MNC. Theorem 5 concludes the conditions or judgments of an algorithm to obtain the MNC. Theorem 6 is given by calculating the number of intersections on each edge light when a deployment achieves the MNC. In other words, theorem 6 is another form of theorem 5 which is on the perspective of the number of intersections on each edge light.

Theorem 6: A deployment achieves the MNC if and only if the number of intersections on each edge light of any j-th sensor is

$$I = \sum_{i=1, i\neq j}^{n} 2m_i + 2$$

where $j = 1, \ldots, n$.

Proof: We prove theorem 6 in its sufficient property and necessary property.

For the sufficient property, if an algorithm achieves the MNC, the three conditions in theorem 5 should be satisfied. For the first condition, any edge light E of any j-th sensor should intersect with all the other edge lights in the FOI, which are not originated from the j-th sensor. There are $\sum_{i=1, i\neq j}^{n} 2m_i$ edge lights in the FOI, except the $2m_j$ edge lights originated from the j-th sensor. For the second condition, no more than two edge lights intersect at the same intersection. Combining the first and second conditions, we find that each of the $\sum_{i=1, i\neq j}^{n} 2m_i$ edge lights generates an intersection on E. For the third condition, no more than one edge light intersects at the same intersection on the boundary of the FOI. In other words, the $\sum_{i=1, i\neq j}^{n} 2m_i$ intersections on E are not on the boundary of the FOI. Since E cuts across the FOI, the boundary of the FOI intersects with E at two intersections. Hence, $I = \sum_{i=1, i\neq j}^{n} 2m_i + 2$, and the sufficient property holds.

For the necessary property, we prove it by contradictions. Suppose that an algorithm cannot obtain the MNC. According to theorem 5, at least one of the three conditions cannot be satisfied. For any edge light E of any j-th sensor, the number of edge lights which are not originated from the j-th sensor is $\sum_{i=1, i\neq j}^{n} 2m_i$. Since E cuts across the FOI, the boundary of the FOI intersects with E at two intersections. There are at most $I_{max} = \sum_{i=1, i\neq j}^{n} 2m_i + 2$ intersections on E. Since at least one of the conditions in theorem 5 cannot be satisfied, we have $I < I_{max}$. This contradicts with $I = I_{max} = \sum_{i=1, i\neq j}^{n} 2m_i + 2$. Hence, the necessary property holds. ■

IV. Experiment Results and Analysis

In experiments, we show that modulators have a significant influence on the number of cells generated in the FOI. For a deployment with n sensors, the j-th sensor is modulated by m_j ($j \in \{1, \ldots, n\}$) modulators. Then, there are n number of variables of m_j. It is difficult to present them in a 3-dimension space. Hence, in experiment I, we set the values of m_j as integers satisfying uniform distribution or being 20 permutation of integers. We study the influence on the MNCs by the statistical property of m_j. Furthermore, in experiment II, we set $m_j = m$, i.e., all the sensors deployed by the same number of modulators to study the influence of modulators on the MNCs and the number of sensors to be deployed. Both experiment I and experiment II are in the environment of Matlab 2017b. In experiment II, we also use our tool proposed in [14].

A. Experiment I: MNC With Varying m and n

In this experiment, we set the values of m_j as integers that are uniformly distributed between 1 and n, i.e., $m_j \sim [1, 20]$. Moreover, we independently repeat the experiments 20 times to observe the number of cells in the FOI when the values of n or m_j vary.

As illustrated in Fig. 3, each ribbon curves the MNCs (or log(MNCs)) varying when the value of n varies from 1 to 20 and the value of m_j satisfies $m_j \sim [1, 20]$. The 20 ribbons represent 20 independent experiments. In Fig. 3(a), we draw the MNCs varying with n in 20 independent experiments and have the following observations. First, intuitively, as the number of sensors increases, the MNCs should increase. In fact,

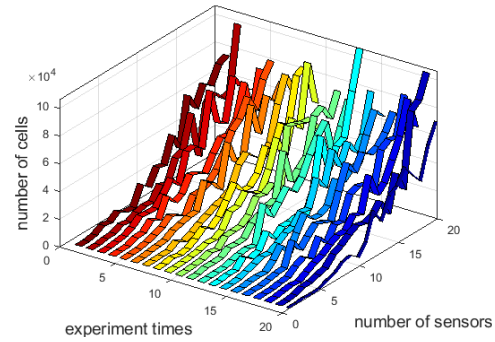

(a) Each ribbon is a list of MNCs for n varying from 1 to 20

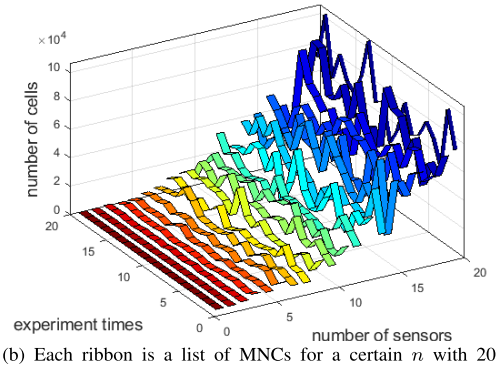

(b) Each ribbon is a list of MNCs for a certain n with 20 experiments

Fig. 3. The MNCs with $m \sim [1, 20]$ and $n \in \{1, \ldots, 20\}$.

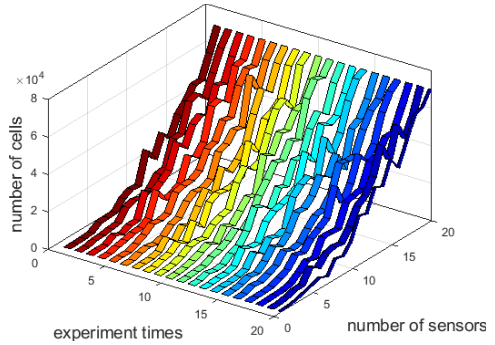

(a) Each ribbon is a list of MNCs for n varying from 1 to 20

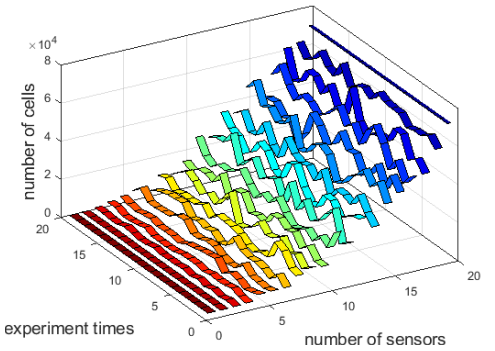

(b) Each ribbon is a list of MNCs for a certain n with 20 experiments

Fig. 4. The MNCs with $n \in \{1, \ldots, 20\}$ and $\{m_1, \ldots, m_n\}$ of each ribbon being a permutation of $n = 20$.

with the values of n varying, all the ribbons have fluctuations due to the MNCs varying. The fluctuations means that when $n_j > n_{j+1}$ $(j + 1 \leq 20)$ and $m_j < m_{j+1}$, the MNCs may have $max(c)|_{n=n_j} < max(c)|_{n=n_{j+1}}$. From the fluctuations, we obtain that both the number of sensors and the number of modulators have a great influence on the MNCs in the FOI. Second, to observe the fluctuation of $0 < n \leq 4$, Fig. 3(b) shows the MNCs for a certain value of n on one ribbon. When $0 < n \leq 4$, it seems that the fluctuation of the MNCs is not obvious. Notice that, the MNCs in z-axis is multiplied by 10^4 and the MNCs are small compared with 1×10^4. In Fig. 3(b), each ribbon represents the MNCs of a certain value of n for the ribbons in Fig. 3(a). Moreover, the fluctuations of the ribbons in Fig. 3(b) are only generated by the values of m_j. In Fig. 3(b), we have two observations. First, as the value of n increases, the fluctuation of each ribbon becomes greater; this means that the more sensors are deployed, the greater the MNC is affected by the number of modulators. Second, the fluctuation of MNC causes the smaller n value to generate more cells than the bigger n value. Since the distribution of m_j is selected as a uniform distribution, we have a question which is whether the fluctuation of the MNCs is influenced by the distribution. Researchers can select a distribution of m_j based on their practical problems.

In order to answer our question from Fig. 3, we let m_j obey a much simpler distribution than the uniform distribution and draw Fig. 4. In Fig. 4, for each ribbon, we set $m_1, \ldots, m_n$ as one of the permutations of $n = 20$ and let n vary from 1 to 20. Moreover, we set $m_1 = 3$ for all the 20 experiments, and this has little influence on the fluctuation of each ribbon. In Fig. 4 (a), we have two observations. First, compared with Fig. 3 (a), the fluctuation in Fig. 4 is much smaller. The reason is that for the permutation of $n = 20$, the range of m_j is much more constrained than that of $m_j \sim [1, 20]$. Second, when $n < 20$, there are fluctuations in each ribbon. But almost all the ribbons achieve the same value of the MNCs when $n = 20$. In order to illustrated this phenomena clearly, we draw the curves in Fig. 4(b), where each ribbon represents the MNCs with the same number of sensors. In Fig. 4(b), we observe that no matter how many fluctuations when $1 < n < 20$, both the ribbons $n = 1$ (as aforementioned, we set $m_1 = 3$) and $n = 20$ are flat. Since each permutation is an arrangement of all the elements in $\{1, \ldots, 20\}$, the $\sum_{j=1}^{n} m_j$ in each permutation of the 20 experiments are the same when $n = 20$.

Comparing Fig. 3 with Fig. 4, we have the following two observations. First, the fluctuations in two figures of Fig. 3 (a) and (b) are greater than the two figures in Fig. 4 (a) and (b), respectively. Second, all the fluctuations in Fig. 4 eventually converge to a certain value when $n = 20$, while the fluctuations in Fig. 3 do not converge. From those observations, we can answer the aforementioned question as follows: the statistical property of m_j influences the MNCs. Moreover, when researchers select the distribution of m_j, the distribution has better to contain some certain property corresponding to their practical problems. For instance, the summation of m_j is a certain value as illustrated in Fig. 4.

B. Experiment II: Spatial Awareness Analysis

In this experiment, the FOI is set as a disc with a radius of 8, each modulator is set as a disc with a radius of 0.004, and the sensors are set as a point. Given the number of sensors, the sensing area size of a sensor is the sensing

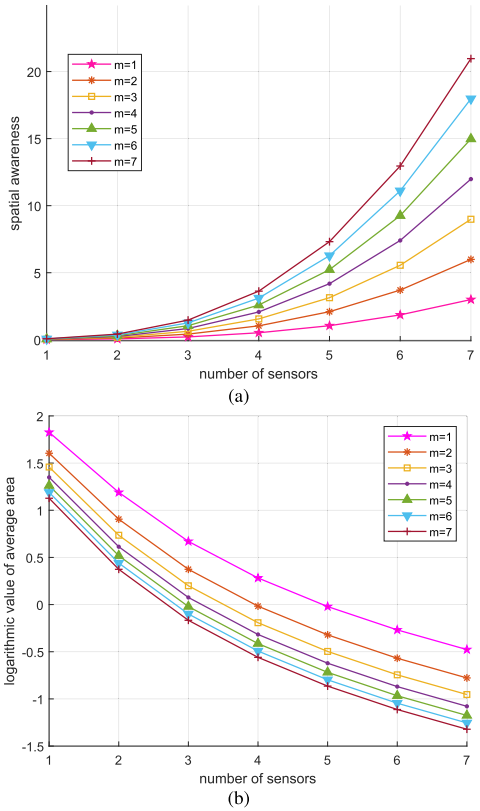

Fig. 5. The spatial awareness under multiple modulators: (a) Spacial awareness under $m_j = m$ and $m \in \{1, 2, 3, 4, 5, 6, 7\}$; (b) The logarithmic of spacial awareness under $m_j = m$ and $m \in \{1, 2, 3, 4, 5, 6, 7\}$.

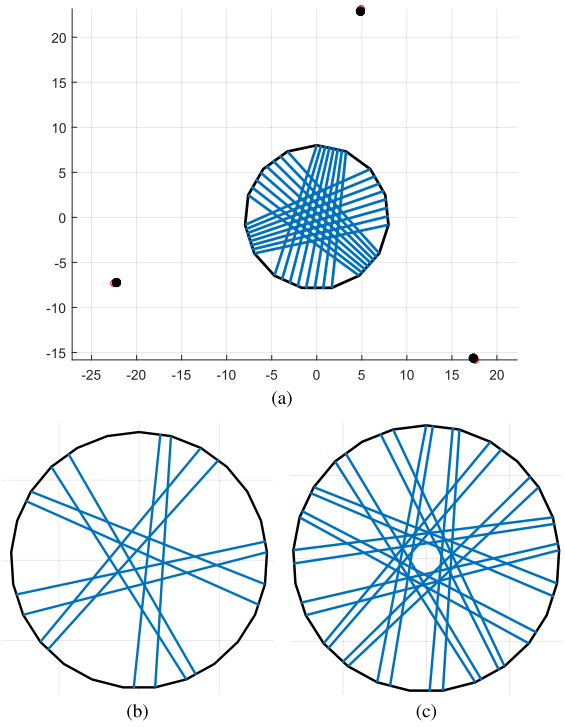

Fig. 6. Segmenting th FOI with multiple modulators; (a) Deployment result of $n = 3$, $m_j = m$ and $m = 4$; (b) Segment result of $n = 5$, $m_j = m$ and $m = 1$; (c) Segment result of $n = 5$, $m_j = m$ and $m = 2$.

accuracy of the sensor system. The spatial awareness of a binary sensor system is defined as follows:

Definition 2: In a binary sensor system, the spatial awareness of a sensor system is denoted as α and $\alpha = c/(\pi R^2)$, where R is the radius of the FOI and c is the number of cells.

Although πR^2 is a constant for a given FOI, the definition of spatial awareness combines the number of cells in the FOI with the average area of cells in the FOI together. Moreover, the definition of spatial awareness is the reciprocal of the average cell area. Actually, the sizes of cells may not be the same. Moreover, some cells may be very large while some other cells are very small as illustrated in Fig. 6

Fig. 5 shows the relationships of the spatial awareness vs. n. In Fig. 5(a), the x-axis is the number of sensors and the y-axis is the value of spatial awareness. We plot seven curves by varying the number of modulators to modulate each sensor from 1 to 7. As illustrated in Fig. 5(a), as the number of sensors increases, the values of spatial awareness increases quickly. Moreover, as the number of sensors increases, the gap of α between every two values of m continues to widen. This means that the monitoring accuracy of the sensor system can be enhanced by either increasing the number of deployed sensors or increasing the number of deployed modulators. When the spatial awareness value is 5 (i.e., $y = 5$), there are several lines in the figure intersecting with $y = 5$. This means that, on one hand, we can achieve a certain spatial awareness by the combinations of different numbers of modulators and sensors. For instance, we can achieve the spatial awareness $y = 5$ by utilizing five sensors (each of them modulated by five modulators) or six sensors (each of them modulated by three modulators). On the other hand, we can utilize more modulators to decrease the number of utilized sensors.

In Fig. 5(b), the x-axis is the number of sensors and the y-axis is the logarithm value of the average cell areas. It is easy to observe that as the number of sensors increases, the spatial awareness approaches to zero very quickly. When there are more than three sensors or four modulators, the average cell area is very close to zero. Then, it is very difficult to deploy sensors and modulators to achieve the MNC because of the cell area being too small. Since many cells have very small cell areas, it is very hard to implement the MNC in practice. Under this condition, a deployment that can segment the FOI into equal size cells should be preferred.

In Fig. 6, the segment results of the FOI with multiple sensors and modulators are shown. In Fig. 6(a), the FOI is segmented by three sensors and each of them is modulated by four sensors. The black dots in the figure are modulators and the red dots are sensors that are placed too close to modulators to see. In Fig. 6(b) and Fig. 6(c), each sensor is modulated by one modulator or two modulators. Moreover, we deploy five sensors in both Fig. 6(b) and Fig. 6(c). To observe the segment results clearly, we omit the locations of the sensors and the modulators. We observe that the intersections are mainly distributed in the middle part of the FOI. The cells, which have a common edge with the BFOI, have a large cell area variance with the cells in the middle part of the FOI. Under a certain spatial awareness, we prefer the deployment that segments the FOI into cells with very small area variances which usually need edge lights are parallel lines. However, two

edge lights tangent with the same modulator always have an intersection angle at the sensor location, which causes the cell area to have a big variance. The angle also makes edge lights difficult to be arranged to achieve the MNC.

V. Related Works

In tracking or localization applications, sensor deployment is an important problem to be studied. Due to the introduction of modulators, the deployment of sensors and modulators is significantly different from the traditional deployment aiming to solve the coverage problem. Researchers design modulators to obtain expected projections of modulators (e.g., the shapes of cells), design the signatures to code cells, and study the performance of cells and signatures.

A. Modulator Design

There are three important factors in modulator design: shapes, sizes, and projection combinations of modulators. The modulator shapes determine the shapes of cells especially in the 3-dimension space; the sizes of modulators determine visible and invisible monitoring regions of sensors; the combinations of modulators limit the number of segmented cells and the values of generated signatures. The authors in [11] study the design limitations of RST and they assert that the placement of sensors and modulators should be uniform to generate a nonsingular matrix of signatures. A tracking system is designed to track the trajectory of a single human [21], where RST separates the omnidirectional view into $\pi/8$ angular parts corresponding to 16 cells. 16 signatures consisted of 8 bits are used to distinguish each cell. A two-column structure is applied to track and identify multi-human: each column spans $2\pi/5$ and is separated into 7 detection areas, and then 14 cells are constructed with 8 signature bits same as [22]. Two kinds of masks: a fan shape and a ring shape, are employed to modulate the view of sensors as RST [5]. They segment the FOI into 16 cells around two adjacent annular regions and one small circle cell in the central zone. Such 17 cells have a similar size but each cell has a unique signature. A six petals torus RST structure is designed to partition the detection range of sensors into 12 distinguished cells [4]. Each petal overlaps with adjacent two petals generating three cells while coding the 12 cells with 12 different signatures. A ring shape modulator is designed with four kinds of masks carved on it [9]. The modulator rotates around a binary sensor while dividing the FOI into 4×3 areas. They measure the shape of a target based on the signal changes while the modulator rotating one round around the sensor. The sensing view of sensors is segmented into 16 cells while each sub-mask is a small disc with holes and occlude some of the 16 cells. Moreover, all of the seven sub-masks are arranged as a circle in a large disc mask. The sub-masks are rotated to modulate the sensing views of sensors.

B. Signature and Cell Design

The studies of signatures and cells can be classified into three aspects: FOI segmentation, the bounds of the numbers of cells or signatures, sensor data process. An integrated framework for binary sensor deployment is proposed for smart home by considering the physical topologies and covering precision constraints [1]. A tool is proposed to obtain the FOI segmentation information such as vertices and signatures of cells and visually present the segmentation results in a computer [14]. The authors in [15], [16] prove the discrimination upper bound (named as spatial resolution) and the achievable discrimination upper bound by regarding binary sensors as a circle to segment the FOI. The researchers provide the upper bound and the lower bound of distinct signatures realized in deployment models [12]. The relationship between the maximum number of signatures and modulators are given in [13], [19], in which they prove that the maximum number of signatures with a certain number of sensors can be achieved by utilizing an unlimited number of modulators to modulate views of the sensors. The optimal placement of both omnidirectional and directional binary sensors are studied in [23], in which they provide the upper bound on the number of unique cells, which are cells bordering on the BFOI. Both signatures and cells are aiming to recognize the target motion. The authors in [10] propose a mining method to find frequent activity patterns by employing activity clustering to group the patterns into activity definitions and a hidden Markov model to represent activities and their variations. A convolutional neural network is utilized to extract activity features hidden behind the time sequence of signatures [8]. Some other feature extraction and activity recognition methods are briefly summarized in [6].

However, there are fewer studies on the MNC. In this paper, we construct a mathematical model of the MNC and propose the sufficient and necessary conditions as the judgment or guide for researchers to design algorithms achieving the MNC. Furthermore, we provide a method to calculate the number of cells when a deployment sometime cannot obtain the MNC.

VI. Conclusion and Future Work

In this paper, we study the MNC of sensor and modulator deployments. We derive a theorem of the MNC and the Euler's Formula is provided to analyze the relationships of edges, intersections, and cells in the FOI. A differential parameter is defined to measure the difference value between the maximum number of intersections, edges, and cells and their actual generated numbers in the FOI. We prove that the maximum numbers of intersections, edges, and cells also satisfy the Euler's Formula, and this means they can achieve their maximum values in one deployment.

We also analyze all the three situations in that deployment cannot achieve the MNC. Based on these three situations, we provide the sufficient and necessary conditions that a deployment can achieve the MNC. Furthermore, we conduct experiments in which the sensors are modulated by a different number of modulators. In experiment I, we study the statistical distribution of the number of modulators to impact the MNCs. In experiment II, we set all the sensors deployed by the same number of modulators to study the influence of modulators on the MNCs and the number of sensors to be deployed achieving a certain spatial awareness. We observe that a certain spatial awareness can be achieved by the combinations of different numbers of modulators and sensors.

Studying the MNC is to deeply understand the binary sensor system with modulators and to help researchers reasonably

select the number of modulators or design more complicated shapes of modulators. We aim to segment the FOI into small cells with small cell area variances. However, the large cell area variance is a problem to be solved. For future work, we will utilize spatial awareness (reciprocal of the average cell area) to obtain the cell area variance and to optimize the value of cell area variance.

REFERENCES

[1] M. P. Fanti, G. Faraut, J.-J. Lesage, and M. Roccotelli, "An integrated framework for binary sensor placement and inhabitants location tracking," *IEEE Trans. Syst., Man, Cybern. Syst.*, vol. 48, no. 1, pp. 154–160, Jan. 2018.

[2] R. A. Nadi and M. G. H. A. Zamil, "A profile based data segmentation for in-home activity recognition," *Int. J. Sensor Netw.*, vol. 29, no. 1, pp. 28–37, 2019.

[3] E. Masazade and A. Kose, "A proportional time allocation algorithm to transmit binary sensor decisions for target tracking in a wireless sensor network," *IEEE Trans. Signal Process.*, vol. 66, no. 1, pp. 86–100, Jan. 2018.

[4] B. Yang and Z. Meng, "Credit-based multiple human location for passive binary pyroelectric infrared sensor tracking system: Free from region partition and classifier," *IEEE Sensors J.*, vol. 16, no. 1, pp. 216–223, Jan. 2017.

[5] X. Luo, Q. Guan, H. Tan, L. Gao, Z. Wang, and X. Y. Luo, "Simultaneous indoor tracking and activity recognition using pyroelectric infrared sensors," *Sensors*, vol. 17, no. 8, pp. 1701–1718, Apr. 2017.

[6] J. Yan, P. Lou, R. Li, and J. Xiong, "Research on the multiple factors influenceing human identification based on pyroelectric infrared sensors," *Sensors*, vol. 18, no. 2, pp. 1–22, Feb. 2018.

[7] W. Zhou, F. Li, D. Li, X. Liu, and B. Li, "A human body positioning system with pyroelectric infrared sensor," *Int. J. Sensor Netw.*, vol. 21, no. 2, pp. 108–115, Jan. 2016.

[8] G. Liu, J. Liang, G. Lan, Q. Hao, and M. Chen, "Convolution neutral network enhanced binary sensor network for human activity recognition," in *Proc. IEEE Sensors*, Oct. 2016, pp. 1–3.

[9] R. Ma, F. Hu, and Q. Hao, "Active compressive sensing via pyroelectric infrared sensor for human situation recognition," *IEEE Trans. Syst., Man, Cybern. Syst.*, vol. 47, no. 12, pp. 3340–3350, Dec. 2017.

[10] P. Rashidi, D. J. Cook, L. B. Holder, and M. Schmitter-Edgecombe, "Discovering activities to recognize and track in a smart environment," *IEEE Trans. Knowl. Data Eng.*, vol. 23, no. 4, pp. 527–539, Apr. 2011.

[11] D. J. Brady, N. P. Pitsianis, and X. Sun, "Reference structure tomography," *J. Opt. Soc. Amer. A, Opt., Image Sci., Vis.*, vol. 21, no. 7, pp. 1140–1147, 2004.

[12] P. K. Agarwal, D. Brady, and J. Matousek, "Segmenting object space by geometric reference structures," *ACM Trans. Sensor Netw.*, vol. 2, no. 4, pp. 455–465, Nov. 2006.

[13] M. Peng and Y. Xiao, "Signature maximization in designing wireless binary pyroelectric sensors," in *Proc. IEEE Global Telecommun. Conf. GLOBECOM*, Dec. 2010, pp. 1–5.

[14] L. Luo, Y. Xiao, W. Liang, and M. Zheng, "A cell reconstruction tool to deploy binary pyroelectric sensor arrays," *IEEE Sensors J.*, vol. 20, no. 4, pp. 2117–2131, Feb. 2020.

[15] N. Shrivastava, R. M. U. Madhow, and S. Suri, "Target tracking with binary proximity sensors: Fundamental limits, minimal descriptions, and algorithms," in *Proc. 4th Int. Conf. Embedded Netw. Sensor Syst. (SenSys)*, 2006, pp. 251–264.

[16] N. Shrivastava, R. Mudumbai, U. Madhow, and S. Suri, "Target tracking with binary proximity sensors," *ACM Trans. Sensor Netw.*, vol. 2, no. 4, pp. 455–465, Nov. 2006.

[17] H. Yang, H. Xu, and K. Tang, "WiHumo: A real-time lightweight indoor human motion detection," *Int. J. Sensor Netw.*, vol. 24, no. 2, pp. 110–117, 2017.

[18] W. Zhuang, Y. Chen, J. Su, B. Wang, and C. Gao, "Design of human activity recognition algorithms basedon a single wearable IMU sensor," *Int. J. Sens. Netw.*, vol. 30, no. 3, pp. 193–206, 2019.

[19] M. Peng, Y. Xiao, N. Li, and X. Liang, "Monitoring space segmentation in deploying sensor arrays," *IEEE Sensors J.*, vol. 14, no. 1, pp. 197–209, Jan. 2014.

[20] D. S. Dief and Y. Gadallah, "Classification of wireless sensor networks deployment techniques," *IEEE Commun. Surveys Tuts.*, vol. 16, no. 2, pp. 834–855, 2nd Quart., 2014.

[21] Q. Hao, D. J. Brady, B. D. Guenther, J. B. Burchett, M. Shankar, and S. Feller, "Human tracking with wireless distributed pyroelectric sensors," *IEEE Sensors J.*, vol. 6, no. 6, pp. 1683–1696, Dec. 2006.

[22] Q. Hao, F. Hu, and Y. Xiao, "Multiple human tracking and identification with wireless distributed pyroelectric sensor systems," *IEEE Syst. J.*, vol. 3, no. 4, pp. 428–439, Dec. 2009.

[23] P. Asadzadeh, L. Kulik, E. Tanin, and A. Wirth, "On optimal arrangements of binary sensors," in *Spatial Information Theory* (Lecture Notes in Computer Science). Berlin, Germany Springer-Verlag, 2011, pp. 168–187. [Online]. Available: https://link.springer.com/chapter/10.1007%2F978-3-642-23196-4_10

[24] S. P. Emmons and F. Kamangar, "Evaluating the optimal placement of binary sensors," *Int. J. Inf. Sci. Techn.*, vol. 3, no. 1, pp. 1–10, Jan. 2013.

[25] B. Poonen and M. Rubinstein, "The number of intersection points made by the diagonals of a regular polygon," Nov. 1997, *arXiv:math/9508209*. [Online]. Available: https://arxiv.org/abs/math/9508209

[26] L. Yuan, Q. Liu, M. Lu, S. Zhou, C. Zhu, and J. Yin, "A highly efficient human activity classification method using mobile data from wearable sensors," *Int. J. Sensor Netw.*, vol. 25, no. 2, pp. 86–92, 2017.

[27] M. Aigner and G. M. Ziegler, "Three applications of Euler's formula," in *Proofs From THE BOOK*. Berlin, Germany: Springer, 2010, pp. 75–80.

[28] R. Diestel, *Graph Theory*. New York, NY, USA: Springer-Verlag, 2000.

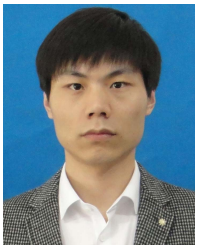

Longxiang Luo (Member, IEEE) received the B.E. degree from Guangxi University, China, in 2012. He is currently pursuing the Ph.D. degree with the Shenyang Institute of Automation, Chinese Academy of Sciences, Shenyang, China. His research interests include sensor deployment and algorithm design, and short packet channel coding.

Yang Xiao (Fellow, IEEE) received the B.S. and M.S. degrees in computational mathematics from Jilin University, Changchun, China, and the M.S. and Ph.D. degrees in computer science and engineering from Wright State University, Dayton, OH, USA. He is currently a Full Professor with the Department of Computer Science, The University of Alabama, Tuscaloosa, AL, USA. He has published over 290 SCI-indexed journal articles, including over 50 IEEE/ACM TRANSACTIONS papers and over 250 EI indexed refereed conference papers and book chapters related to these research areas. His current research interests include cyber-physical systems, the Internet of Things, security, wireless networks, smart grid, and telemedicine. He was a Voting Member of the IEEE 802.11Working Group from 2001 to 2004, involving the IEEE 802.11 (WIFI) standardization work. He is an Fellow of IET (previously IEE). He has been an Editorial Board or an Associate Editor for 20 international journals, including the IEEE TRANSACTIONS ON CYBERNETICS since 2020, IEEE TRANSACTIONS ON SYSTEMS, MAN, AND CYBERNETICS: SYSTEMS from 2014 to 2015, IEEE TRANSACTIONS ON VEHICULAR TECHNOLOGY from 2007 to 2009, and IEEE COMMUNICATIONS SURVEY AND TUTORIALS from 2007 to 2014. He has served as a Guest Editor over 20 times for different international journals, including the IEEE NETWORK, IEEE WIRELESS COMMUNICATIONS, and *ACM/Springer Mobile Networks and Applications* (MONET). He also serves as the Editor-in-Chief for *Cyber-Physical Systems*.

Wei Liang (Senior Member, IEEE) received the Ph.D. degree in mechatronic engineering from the Shenyang Institute of Automation, Chinese Academy of Sciences, Shenyang, China, in 2002. She is currently a Full Professor with the Shenyang Institute of Automation, Chinese Academy of Sciences. As a Primary Participant/a Project Leader, she developed the WIA-PA and WIA-FA standards for industrial wireless networks, which are specified by IEC 62601 and IEC 62948, respectively. Her research interests include industrial wireless sensor networks and wireless body area networks. She received the International Electrotechnical Commission 1906 Award in 2015 as a distinguished expert of industrial wireless network technology and standard.